PROCEEDINGS OF SCIENCE
ONLINE ICRC 2021 THE ASTROPARTICLE PHYSICS CONFERENCE Berlin | Germany
37th International Cosmic Ray Conference 12–23 July 2021

Zenith angle dependence of pressure effect in GRAPES-3 muon telescope

M. Zuberi,[a,*] S. Ahmad,[c] M. Chakraborty,[a] A. Chandra,[c] S.R. Dugad,[a] U.D. Goswami,[l] S.K. Gupta,[a] B. Hariharan,[a] Y. Hayashi,[b] P. Jagadeesan,[a] A. Jain,[a] P. Jain,[d] S. Kawakami,[b] H. Kojima,[e] S. Mahapatra,[i] P.K. Mohanty,[a] R. Moharana,[j] Y. Muraki,[g] P.K. Nayak,[a] T. Nonaka,[h] A. Oshima,[e] B.P. Pant,[j] D. Pattanaik,[a,i] G. Pradhan,[k] P.S. Rakshe,[a] M. Rameez,[a] K. Ramesh,[a] L.V. Reddy,[a] R. Sahoo,[k] R. Scaria,[k] S. Shibata,[e] K. Tanaka[f] and F. Varsi[d] [The GRAPES-3 Collaboration]

[a] *Tata Institute of Fundamental Research, Homi Bhabha Road, Mumbai 400005, India*
[b] *Graduate School of Science, Osaka City University, Osaka 558-8585, Japan*
[c] *Aligarh Muslim University, Aligarh 202002, India*
[d] *Indian Institute of Technology Kanpur, Kanpur 208016, India*
[e] *College of Engineering, Chubu University, Kasugai, Aichi 487-8501, Japan*
[f] *Graduate School of Information Sciences, Hiroshima City University, Hiroshima 731-3194, Japan*
[g] *Institute for Space-Earth Environmental Research, Nagoya University, Nagoya 464-8601, Japan*
[h] *Institute for Cosmic Ray Research, Tokyo University, Kashiwa, Chiba 277-8582, Japan*
[i] *Utkal University, Bhubaneshwar 751004, India*
[j] *Indian Institute of Technology Jodhpur, Jodhpur 342037, India*
[k] *Indian Institute of Technology Indore, Indore 453552, India*
[l] *Dibrugarh University, Dibrugarh 786004, India*

E-mail: meeran.zuberihep@gmail.com

A large area (560 m^2) muon telescope in the GRAPES-3 experiment at Ooty, India records muon intensity at high cutoff rigidities (R_C) varies from 14–32 GV along 169 independent directions spanning a field of view of 2.3 sr. The threshold energy of the recorded muons is sec(θ) GeV along a direction with a zenith angle (θ) and with the average angular accuracy of $\sim 4^o$. The directional capabilities of the muon telescope are exploited for studying the effect of atmospheric pressure on the muon flux as a function of R_C. It is observed that the barometric coefficients relationship with logarithmic R_C can be well described by second order polynomial function with a high Spearman Rank correlation coefficient of 0.99.

37th International Cosmic Ray Conference (ICRC 2021)
July 12th – 23rd, 2021
Online – Berlin, Germany

*Presenter

1. Introduction

The cosmic rays are the charge particles (mostly protons) that hit the Earth atmosphere almost isotropically. When a primary cosmic ray approach the Earth, it firstly interact with the Earth magnetic field (GMF) where it experiences the deflection depending on its rigidity. Afterwards, the primary cosmic ray continues to move towards Earth surface and interacts with the Earth atmospheric nuclei and produces the secondaries including muons and neutrons. Therefore, any change in atmospheric condition such as pressure or temperature can influence the observed cosmic ray flux at detector level [1, 2]. These atmospheric effects on cosmic rays are known from several decades. There are several studies by various experiments for studying the effects of atmospheric pressure (barometric effect) [3, 4] and temperature [1, 5] on cosmic rays, which shows that these effects can produce the significant modulations in the cosmic ray flux at detector level. Hence, the correction of these effects becomes necessary for doing the precision measurements.

The barometric effect is directly related to the production, decay, or absorption of secondaries in the Earth atmosphere. The probability of these processes depend on the energy of primary particles. It is expected that higher energy primary particle will produce the higher energy secondaries, which will be lesser affected by the changes in the atmospheric pressure. Therefore, the energy dependence of atmospheric effect on secondaries can be utilise to study the relationship with geomagnetic cutoff rigidities of primaries, which quantifies the minimum energy required by a primary particle to reach that location. There are very few studies that explores the relationship of barometric coefficient with cutoff rigidities by using muons[6, 7]. However, these studies are limited up to ~25 GV cutoff rigidities wheres, the GRAPES-3 Muon telescope directional rigidities vary from ~14 GV to ~32 GV, which gives a unique advantage to study this phenomena in the higher rigidity ranges.

2. The GRAPES-3 muon telescope (G3MT)

The muon component of EAS plays a vital role in the field of cosmic rays astrophysics by distinguishing between γ–ray primary from charged cosmic rays particles. It allows to do the search for cosmic ray sources through γ—ray astronomy and studies on the variation of the nuclear composition of primary cosmic rays. The GRAPES–3 experiment has a 560 m^2 G3MT which can give not only the information of muon content in an shower but also the directional information of individual muons. The G3MT comprises of 16 identical modules of 35 m^2 sensitive area each using proportional counters (PRCs) as the basic building block. The PRC is a 6 m long, mild–steel, square pipe, with the cross–sectional area of 10 cm × 10 cm and a wall thickness of 2.3 mm. Each module consists of 232 PRCs arranged in 4 layers. The alternate layers are placed in an orthogonal direction to track the muon in 2 D plane. Two successive layers of PRCs are separated by a concrete block of $60 \times 60 \times 15\, cm^3$. There are total 15 layers of concrete deployed from bottom layer of PRCs which gives a total thickness of 550 g cm^2 which corresponds to a threshold of 1 GeV for vertically incident muons. These concrete blocks are arranged in an inverted pyramid shape to achieve an energy threshold of 1 (secθ) GeV for muons incident on the detector at a zenith angle θ with coverage up to 45^o. The muon angle data is grouped into the $13 \times 13 = 169$ out of 225 bins restricting the maximum zenith angle up to 50^o which still exceeds the shielding coverage of 45^o [8] as shown in Fig. 2.

The unique capability of directional reconstruction of the G3MT also permits to explore various transient phenomenon like geomagnetic storms [9, 10], acceleration of particles during thunderstorms [11], etc. The effective cutoff rigidities in 169 directions are numerically calculated by using back-tracing algorithm [12] as shown in Fig. 2. The details of the cutoff rigidity calculation can be found elsewhere [13].

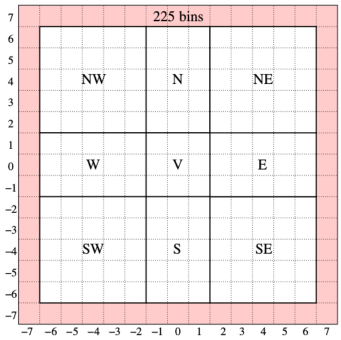

225 angular bins

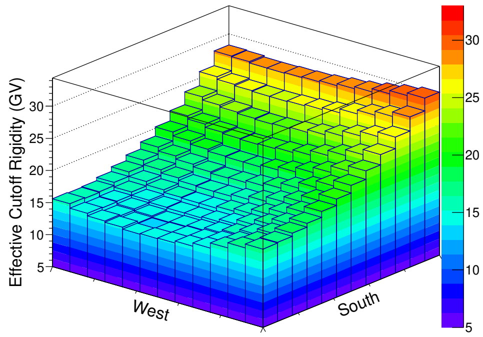

R_C variation in 2-D space

3. Barometric coefficient calculation

The modulation in the atmospheric pressure changes the mass of the air column above the detector which causes the variation in secondary cosmic ray flux. However, the measured flux variation is also coupled with various solar phenomenon which need to be isolated before studying the barometric effect. The Fast Fourier Transform (FFT) technique is used to segregate both these effects [14]. The power spectrum of (A) muon angle data for a particular direction 083, and (B) atmospheric pressure is shown in Fig.1 for combined six years (2001-2006) of data.

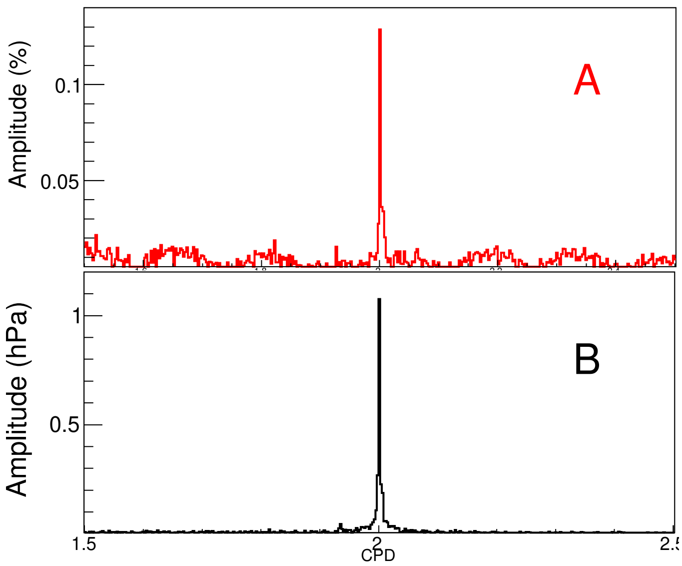

Figure 1: Power spectrum of (A) muon angle, and (B) atmospheric pressure

Both the data sets show a dominant peak at 2 cycle per day (cpd), which is expected due to pressure effect. We have designed a band pass filter to select the frequency centered at 2 cpd from both the data sets and then performed Inverse Fast Fourier Transform (IFFT) on the filtered frequency components to convert them back into the time series data. The % change in filtered muon data is plotted against the change in filtered atmospheric pressure from its mean value, which shows a very strong anti-correlation pattern for all 169 directions. We have used the linear regression technique to determine the barometric coefficient (β_P) for all 169 directions by using the following equation:

$$\frac{\Delta I}{<I>} (\%) = \beta_P \text{ (P -<P>)}$$

The Fig.2 shows the variation for a particular direction 083. The β_P is found to be -0.18%/hPa wih high value of Pearson correlation coefficient of 0.99.

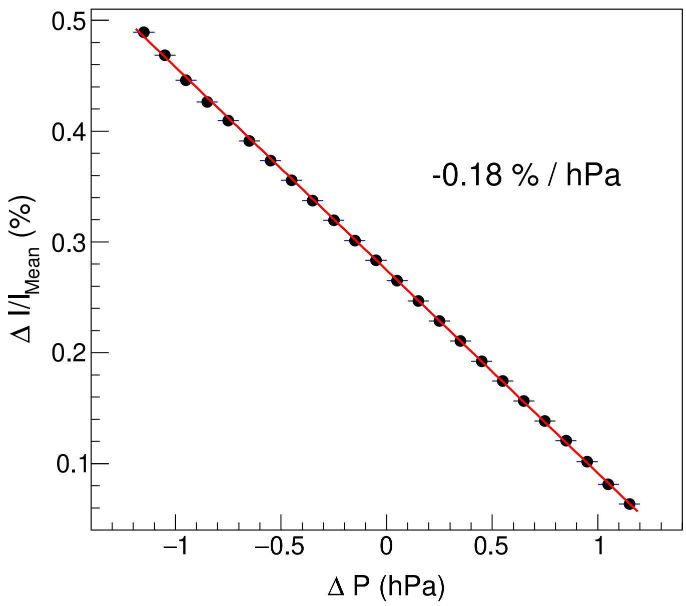

Figure 2: Change in muon flux (%) vs atmospheric pressure

The Fig.3 shows the variation of β_P for all 169 directions in 2-D space. It is evident from the Fig.3 that the value of β_P is more in western direction as compare to the eastern ones.

4. Barometric coefficient dependence on R_C

The east-west asymmetry observed in β_P resembles that seen in case of R_C. The Fig.4 shows the variation of β_P as function of natural logarithmic of R_C.

It is observed that the the value of β_P decreases linearly with increase in ln(R_C) up to R_C ~25 GV, beyond which the curve seems to get flatten. Both these features can be well modeled by a second order polynomial fit, which yields the coefficient values of p0 = -1.28 ± 0.08, p1 = 0.57 ± 0.05, and p2 = -0.06 ± 0.01. The Spearman Rank correlation coefficient value is found to be 0.99, which shows the tight relationship between these two variables.

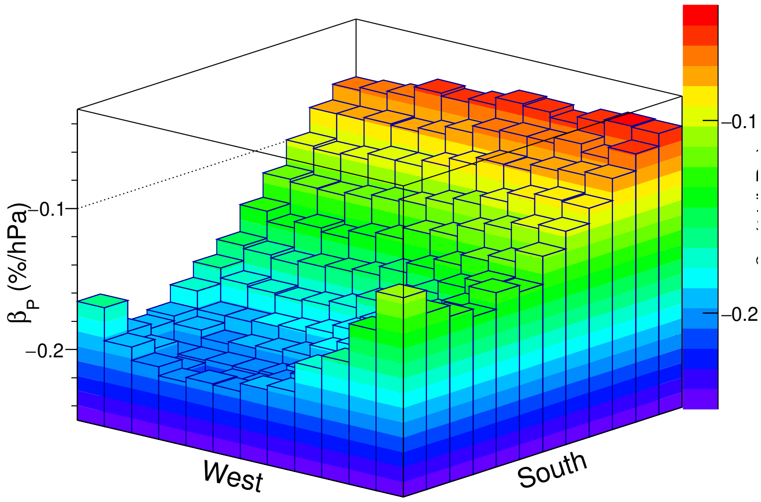

Figure 3: Variation of β_P for all 169 directions in 2-D space

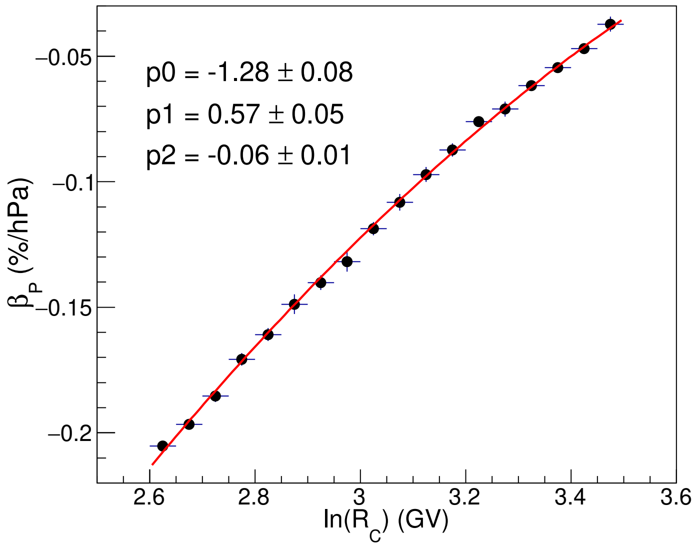

Figure 4: Variation of β_P as a function of ln(R$_C$)

5. Conclusions

In this study we observed a strong correlation between muon and the atmospheric pressure all 169 viewing directions of G3MT. The barometric coefficients are obtained with the aid of FFT technique. The large cutoff rigidity variation (14 GV to 32 GV) distributed among 169 directions are exploited to study the rigidity dependence of barometric coefficients. The coefficients show a tight relationship with the natural logarithmic of rigidities with a high Spearman Rank correlation coefficient of 0.99. The barometric coefficient was expected to show a linear relationship with

$\ln(R_C)$ but a clear departure from the linear trend can be seen at R_C ~25 GV, which can be fitted well with the second order polynomial. However, to understand the possible physical mechanisms responsible for this peculiar behavior of β_P further work is needed.

References

[1] Dorman, L. I., Astrophysics and Space Science Library. Netherlands, Dordrecht: Springer (2004)

[2] Sagisaka, S., Il Nuovo Cimento C, 9(4), 809–828 (1986)

[3] Ambrosio, M., et al., Astroparticle Phys., 7(1–2), 109-124 (1997).

[4] Adamson, P., et al., Phys. Rev., D(81), 012001, (2010).

[5] Arunbabu, K. P., Astroparticle Physics 94, 22–28 (2017).

[6] Mendonca RRS et al., J Geophys Res: Space Phys 124(12) 9791–9813 (2019)

[7] Maghrabi et al., Advances in Astronomy, vol. https://doi.org/10.1155/2016/9620189 (2016)

[8] Y. Hayashi et al., Nucl. Instrum. Methods A 545, 643 (2005).

[9] P.K. Mohanty et al., Phys. Rev. Lett. 117, 171101 (2016).

[10] P.K. Mohanty et al., Phys. Rev. D 97, 082001 (2018).

[11] B. Hariharan et al., Phys. Rev. Lett. 122, 105101 (2019).

[12] Smart, D.F., Shea, M.A., Adv.Space Res.36, 2012 (2005)

[13] B. Hariharan et al., Experimental Astronomy 48, 111–120 (2019)

[14] P.K. Mohanty et al., Astropart. Phys. 79, 23–30 (2016).